SOLVING THE RADIATION PROBLEM IN THE TIME DOMAIN WITH A PANEL METHOD

TYLER COLE

Solving the Radiation Problem in the Time Domain with a Panel Method

by

©Tyler Cole, B.Eng.

A thesis submitted to the School of Graduate Studies

in partial fulfillment of the requirements for the

degree of Master of Engineering

Faculty of Engineering and Applied Science

Memorial University of Newfoundland

August, 2011

St. John's Newfoundland Canada

Abstract

In the present study a linear boundary value solution for the ship wave radiation problem at zero speed and at forward speed is obtained in the time domain. Fluid velocity potentials due to the non-impulsive input and constant input are obtained by solving the boundary value problem using source strengths (indirect method). The singularities in the Rankine source of the transit free surface Green function were dealt with by the use of the well known Hess-Smith method. The panel method was validated by the application of the classical problem of the hemisphere and extended to the application of the Wigley Hull for the radiation problems at forward speed. The computed response functions, added-mass and damping coefficients, along with the wave resistances were compared with published results. The final part of this thesis discusses some of the limitations of the Green function and suggest numerous ways to avoid these intrinsic errors.

Acknowledgments

First and foremost I want to express my thanks to my supervisor, Dr. Wei Qiu, for his advice and guidance throughout the progress of my research. I would also like to thank Dr. Shaoyu Ni, a post doctorate of Dr. Qiu for his extensive help and encouragement. It has been a great opportunity to work with Dr. Wei Qiu and the Advanced Marine Hydrodynamics Lab group during the development of this work. A great deal of knowledge on mathematics and computational hydrodynamics was gained during my time here.

I would like to acknowledge my friend Evan Martin who provided me with his help during my research. Lastly, I would like to thank my family for all their love and encouragement. I would like to mention my mother, Lily Cole and my girlfriend, Karen Pike, because without their support, this thesis would not be possible and my late father, Kenneth Penney, who encouraged me to pursue my academic career.

Contents

List of Figures

Nomenclature

$F(P,Q,t-\tau)$	Memory part of the Green function
$G(P,Q,t-\tau)$	Time-Domain Green function
$G_0(P,Q)=(\frac{1}{r}-\frac{1}{r'})$	Rankine Source
$H(t-\tau)$	Heaviside unit step function
J_0	Bessel function of order Zero
K_{jk}^R	Response function for the radiation force in k^{th} degree of freedom(N)
K_j^D	Response function for the diffraction force
$P(P,t)$	Pressure at a point P at time t(Pa)
$S_B(t)$	Instantaneous wetted surface of the body
$S_{\bar{B}}$	Mean wetted surface of the body
S_{Bottom}	Bottom of the fluid domain
S_F	Free surface
S_∞	Boundary at infinity
U_0	Forward speed of body $(\frac{m}{s})$
V	Fluid domain
$V_n(P,t)$	Normal velocity at point P at time t
$\vec{W}$	Steady flow velocity vector
b_{jk}	Time independent hydrodynamic damping coefficient of the floating body
c_{jk}	Time independent hydrodynamic restoring force of the floating body
g	Acceleration due to gravity $(\frac{m}{s^2})$
m_k	M-terms that are the gradients of the steady velocity in the normal directic
$\vec{n}$	Normal Vector point into the body
r_1, r	Distance between source and field points
$\vec{r}_{cg}$	Position vector for center of gravity

t	Time
t_0	Initial time
Γ	Intersection of body surface and mean water plane
$\Phi(p,t)$	Total velocity potential at any point P(x,y,z) at time t
α	Arbitrary constant which controls the non-impulsive input
$\delta(t)$	Dirac Delta function
$\dot{\eta}(t)$	Non-impulsive velocity input
μ_{jk}	Time independent added-mass of the floating body
ρ	Fluid density($\frac{kg}{m^3}$)
$\sigma(Q,\tau)$	Source strength for point Q at time τ
ϕ_k	Velocity potential for radiated wave in the k^{th} degree of freedom
ϕ_7	Velocity potential for diffracted wave
$\phi_k, \varphi_k, \bar{X}_k$	Components of radiated potential due to decomposition

Chapter 1

Introduction

With an expected increase in industrial activities in the Arctic, interest in ice loads on ships and offshore structures is again becoming an important engineering research topic. The $STePS^2$ Research Project, a relatively large, multi-faceted, research undertaking at Memorial University was created, to better quantify ice loads experienced by ships and structures operating in arctic waters. One of the ice loading scenarios, to be investigated by the $STePS^2$, project is the interaction between a moving ship and relatively small ice masses floating in the path of the vessel. Such impacts can be a significant driver of structural design or a significant source of operating risk. A promising method of understanding and predicting such interaction scenarios is the numerical modeling of the hydrodynamic interaction between a vessel and a small ice piece when the vessel is underway. The first step in developing a complete numerical model of this interaction scenario is to understand and quantify the hydrodynamic pressures and forces for the ship undergoing forward motion at a constant speed.

The intent of the work detailed in this thesis is to develop an efficient but relatively simple hydrodynamic model of a ship at forward speed that can be used as the first step in developing a full simulation model of the ship-ice interaction scenario.

In developing this model, a Boundary Element Method (BEM), or Panel Method, was considered as a reasonable first step. The panel method is based on potential flow theory. This was done on the premise that the interaction problem is primarily influenced by pressure forces and thus the viscous effects need not be modeled at this stage. The intent is to create a relatively simple and robust numerical tool to accurately predict the coefficients of added mass and damping, as well as the wave making resistance of hull forms using a transient free surface Green function. The primary technical challenge is solving the Green function to provide the numerical prediction of coefficients of added mass and damping and the wave making resistance of a ship under forward speed.

As an alternative approach, predictions can be made by physical model tests. However current advancements in computing power and computational tools make numerical prediction a viable alternative to conventional model tests. Numerical methods are becoming more cost effective due to their lower cost and quicker computing time. On the other hand, more complex numerical methods are also available for marine hydrodynamic predictions such as solutions based on the Reynolds-Average-Navier-Stokes (RANS) equations, Large Eddy Simulation (LES), and Direct Numerical Simulation (DNS). These methods all solve the Navier-Stokes equations for fluid mechanics and are known as Computational Fluid Dynamic (CFD) codes. These codes include the effects of viscosity but are complex and time consuming, both in problem definition and in code execution, when compared to the simple Panel Method approach. It may however be possible, once the potential flow model is completed, to upgrade the model to include viscous effects. However, at this stage, it was considered a better approach to start with a simple model that explores the primary effects.

In summary, the overall purpose of this study is to develop a Boundary Element Method based prediction code using the Green function to solve the radiation problems in the time domain. The layout of the thesis following this introductory section is as follows. The remainder of Chapter 1 presents the current state of the art in hydrodynamic modeling using the panel method. Chapter 2 presents the mathematical formulation of the boundary value problem. Chapter 3 discusses the solution based on the impulse response function in order to solve for coefficients of added-mass and damping. The numerical implementation of the equations is outlined in Chapter 4. In Chapter 5 the numerical solutions are compared with experimental results and published numerical results. The limitations of the Green function and how to appropriately apply the function for reasonable results are also discussed in Chapter 5. Conclusions and recommendations for future numerical development are presented in Chapter 6.

1.1 Previous Work

The following sections detail the development of various aspects of the modeling problem covering the numerical approaches and the evolution of the panel method, starting with basic radiation problems and moving through early strip theory and frequency domain approaches to the development of more accurate panel methods in the frequency domain and panel methods for time domain analysis.

1.1.1 Radiation Problems

The radiation problem covers the modeling of waves radiated by a moving or oscillating body on the free surface of a fluid. Solution of this problem underpins both the wave resistance model and general sea keeping models. For this reason reference

is made to both problems in the following sections.

The specific application of the radiation problem for this case is the wave making resistance, which is a form of drag created by an object moving on a fluid free surface. It is a direct reflection of the amount of energy that is required to displace the fluid in front of the object. This energy is an irrecoverable expenditure and leaves the system as a radiated wave. The wave making resistance is highly dependent on the speed to length ratio of the ship. In deep water, the wave system speed is equal to the ships speed. This results in an initial near linear relationship between ship speed and wave making resistance, until a limiting point at which the wave resistance dramatically increases. This limiting point is approximately a Froude number of 0.415 however most displacement hull forms operate at a speed-length ratio larger than 1 according to Savitsky (2003). The first attempt to numerically predict the wave making resistance of a surface ship was by Michell (1898) late in the nineteenth century. Tuck (1964) further examined Michell's work with traditional strip theory, which implies two-dimensional flow on all sections. However two-dimensional transverse flow does not provide an adequate model for flows at forward speed, but is more suitable for zero or low speed seakeeping predicitions. Because of its ability to better model the flow conditions for forward speed, most researchers prefer to use the panel method to determine the wave making resistance, Newman (1979) and Annelsland (1986).

There have been many challenges in accurately predicting ship resistance. For wave making resistance, the floating body must have a forward speed which results in the Neumann-Kelvin problem (Newman, 1977). This increases the complexity of the solution due to the required Green function. Ogilvie (1964) and Cummins (1962) attempted to directly formulate the problem in the time-domain using a time-dependent Green function. This approach was further examined by Wehausen (1971)

for zero forward speed. Recently, Kim, et al. (1998) have predicted wave making resistance using a higher order panel method. Lee, et al. (1997) used a B-Spline panel method to create a more efficient and robust solution to the wave making problem.

1.1.2 Frequency-Domain Solution

In the frequency domain, problems are linearized based on assumptions that the motions are small and time-harmonic, coupled with the use of the mean wetted surface on the body. This method has been very successful for zero forward speed problems (Korsmeyer, et al. 1988). According to Lin & Yue (1991) they have become an industry standard tool for the design of large offshore structures. Chang (1977) and Inglis and Price (1982) attempted to formulate the problem with non zero forward speed, using a zero-speed frequency domain Green function with a speed adjustment. The presented results only had meaning if the body motions were sinusoidal in time. This coupled with the difficulties in the computation of the Green function with the speed adjustment in the frequency domain, an alternative method was desired. The suggested alternative approach was to solve the problem directly in the time-domain.

1.1.3 Linear Time-Domain Solution

Due to the difficulties of the basic frequency-domain solution, many attempts have been made to refine the approach, with limited success according to Lin & Yue(1991). To overcome the difficulties, Cummins (1962) and Ogilvie (1964) moved to solve the zero-forward speed problem directly in the time-domain with a linear free surface, expanding on the work of Finkelstein (1957) and Stoker (1957). The linear radiation problem was solved by using the unit impulse response function, which provides the coefficients of added mass and damping for the body under consideration. The unit response function describes the body's response to an unit impulse motion in any

degree of freedom. The implusive motion of the body gives rise to a force from the surrounding fluid which can be resolved into added mass and linear damping coefficients. Cummins (1962) states that a solution for this unit impulse response provides the basis for a solution to the body response to an arbitrary force by providing the coefficients of added-mass and damping which can be applied to the more general motion cases.

Wehausen (1971) furthered this research for the zero forward speed case with extensive analysis of the problem, presenting detailed results (Wehausen 1971, 1967). Consistent two-dimensional (strip theory) time domain results have been available for some time, however three-dimensional (panel) results are still variable. The first three-dimensional time-domain problems were linearized in an attempt to reduce the mathematical and numerical complexity.

In linear time-domain formulations, the time-dependent Green function is applied to derive a boundary intergral equation at the mean wetted body surface, assuming that the body's wetted surface area does not change, i.e., the mean wetted surface is used and motions are assumed to be small in amplitude. In this study the linear radiation forces acting on the body then are expressed by convolution integrals with impulse functions. Newman (1985) successfully computed the impulse response function for a cylinder in the time-domain, satisfying the zero-speed case. However, the non-zero speed formulation was of greater practical interest. Liapis (1986) and King (1987) furthered the time-domain analysis method by developing a non-zero forward speed solution. They developed a fully three-dimensional mathematical problem for time-domain analysis for a constant forward speed, creating a large leap forward in time-domain simulation. The next progression in time domain analysis was the ability to include varying forward speed, large amplitude waves and a non-linear free surface

condition, which covers most realistic cases.

A variation of the method was introduced by Dawson (1977). Dawson introduced panels on the free-surface, as well as the body surface using Rankine sources to satisfy the free-surface condition. This approach is known as a quasi-linearized free surface. Recent results have been promising for this method, due to its development for many years by others: Larsson (1987) and Nakos & Sclavounos (1990). Lin and Yue (1991) state that in this method the free surface and body geometry remain fixed in the undisturbed positions, and the nonlinearities of the geometry are not included.

1.1.4 Nonlinear Time-Domain Solution

Current research has been carried out to include nonlinearity into the time-domain formulation. Lin & Yue (1991), and Beck & Magee (1990) have extended the time-domain approach to arbitrary large-amplitude motions. The free surface however remained linear so that the time-dependent Green function can still be applied. This was achieved by applying the body boundary condition on the instantaneous submerged hull surface. This has been referred to as the body exact problem. Qiu, et al. (2006) achieved this, using a panel free method and applying the body boundary condition on the instantaneous submerged hull surface. Following researchers have had various success with this formulation. Qiu & Peng (2007) used a the panel free method to combine the exact body boundary conition with a free surface condition linearized about the incident wave profile. The presented results showed improvement for cases of computations dealing with large-amplitude motions.

The final progression in the time-domain formulation is to include the nonlinear free surface. With the Green function the free surface must maintain linearity, limiting the ability of the method to include significant nonlinear wave effects. This poses limitations on the panel method with researchers such as Song (1993) attempting to use the Rankine Source method as an alternative approach to satisfy the nonlinear free surface.

In summary, the current state-of-the-art methods are higher order panel methods using either the Rankine panel or the Green function method. Higher order Rankine panel methods are fully nonlinear, as they include the nonlinear free surface using various numerical techniques. Huang and Sclavounos (1997) addressed the nonlinear free-surface using weak-scatterer theory, linearizing the ship wave disturbance about the instantaneous position of the ambient wave problem. The nonlinear wave resistance results were an improvement over the standard linear theory when compared to experimental results. These predictions are still not fully nonlinear. Kim, et al. (2011) also used the weak-scatter theory approach showing similar results. Broeze, et al. (1993) developed a higher order three-dimensional Rankine panel method for non-linear free surface waves. They claim that the results were stable and accurate. However, due to the complexity of the numerical scheme, a vector supercomputer was required for the computations to deal with the motion of the grid. For the Green function method, higher order results are almost fully non-linear. The only limitation of the Green function, is that the free surface must maintain is linearity. This method is called the blended approach. The body boundary condition is applied to the instantaneous wetted surface, known as the body-exact problem, but the free-surface still remains linear. Qiu & Peng (2007) achieved this with a panel free approach. However, without the inclusion of the nonlinear free surface, the method is still limited, due to

the slight reduction in accuracy (Lin & Yue 1991).

In this work, the Green function approach was choosen, in which the linear free surface boundary condition is satisfied on the free surface and the linear body boundary conditions are satisfied on the mean wetted body surface.

Chapter 2

Mathematical Formulation

2.1 Boundary Value Problem

In setting up the problem based on the work of Liapis (1986) the following conventions and boundary conditions are used. Figure 1 shows a coordinate system and the boundaries used to define the boundary value problem. The local coordinate system is fixed to the floating ship at the center of the midship, moving in the positive x-axis with a constant forward speed of U_0. The x coordinate is positive in the direction of the bow, the y coordinate is positive in the direction port, while the z coordinate is positive upward. The boundaries seen in Figure 1 are the free surface (S_f), body's surface (S_B), bottom surface (S_{bottom}), and the conditions at infinity (S_∞). Each boundary must satisfy its own individual boundary condition. When using potential flow theory, the fluid is assumed to be incompressible, inviscid, free of surface tension, and irrotational. With these assumptions, coupled with the assumption of small unsteady oscillations, a velocity potential Φ can exist at any time t where the velocity of the fluid can be described at any point P(x,y,z) at the corresponding time by the

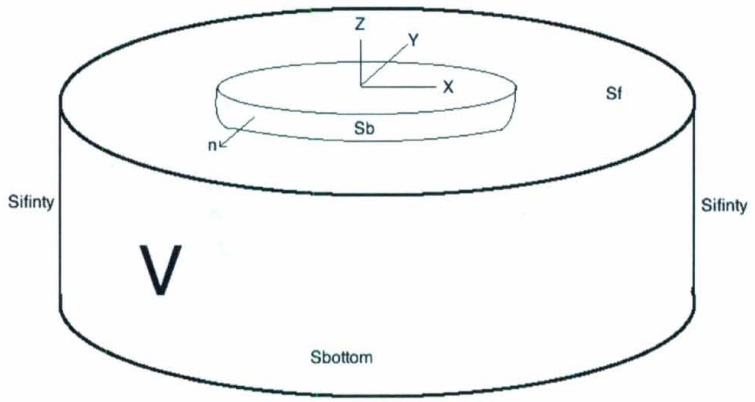

Figure 2.1: Boundary Value Problem Domain and Coordinate System

gradient of the potential given by:

$$V(P;t) = \nabla\Phi(P;t). \tag{2.1}$$

With this defined potential, the boundary condition must be enforced on all boundaries and can be defined mathematically. The governing equation is the Laplace equation, (Equation 2.2) which stipulates the conservation of mass in the entire bounded volume V.

$$\nabla^2\Phi(P;t) = 0. \tag{2.2}$$

The fluid must satisfy the body boundary condition, known as the "no-flux" boundary condition, given by:

$$(\nabla\phi - \vec{V_s}) \cdot \vec{n} = 0, \quad \text{on} \quad S_b, \tag{2.3}$$

meaning no fluid will flow cross the body boundary. S_b is the mean wetted body surface and does not change with time where $\vec{n}$ is the unit out-ward normal vector, pointing out of the body. On the free surface, the exact boundary condition is derived from Bernoulli's equation assuming that the surface tension and viscous effects are

negligible. The exact (non-linear) boundary condition can be written as,

$$\frac{\partial^2\phi}{\partial t^2} + 2\nabla\phi\cdot\nabla\frac{\partial\phi}{\partial t} + \frac{1}{2}\nabla\phi\cdot\nabla(\nabla\phi\cdot\nabla\phi) + g\frac{\partial\phi}{\partial z_0} = 0, \quad \text{on} \quad z = \eta. \tag{2.4}$$

where $\eta(x_0, y_0, t)$ is the unknown wave elevation (or amplitude) and (x_0, y_0, z_0) defines a point on the free surface.

On the bottom boundary it is assumed that fluid velocity effects from the body vanish, represented by:

$$\lim_{r\to\infty} \nabla\phi(P,t)\Big|_{z=-d} = 0, \quad \text{on} \quad S_{\text{bottom}}. \tag{2.5}$$

The conditions at infinity are known as the Sommerfield radiation conditions that state waves created by the floating body propagate away from the body and vanish in the far field S_∞ given by:

$$\lim_{r\to\infty} \frac{\partial\phi}{\partial y}\Big|_{z=\pm d} = 0, \quad \text{on} \quad S_\infty. \tag{2.6}$$

With the above boundary conditions, a linearized problem can be set up to allow the application of superposition, greatly simplifying the problem. If the disturbances in the fluid are small in the steady problem and in the unsteady problem, both can be separated due to the principles of superposition, allowing the following breakdown of the total velocity potential:

$$\Phi(P;t) = -U_0X + \phi_0(x,y,z) + \phi_t(x,y,z;t), \tag{2.7}$$

where $-U_0X$ and ϕ_0 are the components that make up the steady effects of the velocity potential while ϕ_t contains all the unsteady effects. The unsteady velocity potential

can later be broken down into the radiation and diffraction potentials (Equation 2.9), where ϕ_k represents all six degrees of freedom and ϕ_D represents the potential of diffracted waves. The total potential can be defined as:

$$\phi_t = \sum_{k=1}^{6} \phi_k(P;t) + \phi_D(P;t). \tag{2.8}$$

The final linearization applied to the boundary value problem, known as the Neumann-Kelvin problem, defines the pressure, free-surface condition and body boundary condition by the following conditions

$$p = -\rho(\frac{\partial \phi_k}{\partial t} - U_0 \frac{\partial \phi_k}{\partial x}), \tag{2.9}$$

$$(\frac{\partial}{\partial t} - U_0 \frac{\partial}{\partial x})^2 \phi_k + g\frac{\partial \phi_k}{\partial z} = 0, \quad \text{on} \quad S_f; \tag{2.10}$$

$$\frac{\partial \phi_k}{\partial n} = n_k \dot{\zeta}_k + m_k \zeta_k, \quad \text{on} \quad S_b; \tag{2.11}$$

where $\vec{n_k}$ is the generalized unit normal is defined by Equations 2.12 and 2.13 and ζ is the amplitude of the unsteady motion in all degrees of freedom.

$$\vec{n} = (n_1, n_2, n_3), \tag{2.12}$$

$$\vec{r} \times \vec{n} = (n_4, n_5, n_6), \tag{2.13}$$

$$\vec{r} = (x_g, y_g, z_g). \tag{2.14}$$

The steady effects and unsteady effects are linked together through the m-terms in the body boundary condition (Newman, 1977). These terms are the gradients of the

steady velocities in the normal direction given by:

$$-(\vec{n}\cdot\nabla)\vec{W} = (m_1, m_2, m_3), \tag{2.15}$$

$$-(\vec{n}\cdot\nabla)(\vec{r}\times\vec{W}) = (m_4, m_5, m_6). \tag{2.16}$$

In the Neumann-Kelvin problem $\vec{W} = -U_0\hat{i}$, coupled with the assumption that the body is slender, and the perturbation of the steady flow field caused by the ship is neglected, the m-terms are simplified to the format represented by:

$$\vec{m} = (0, 0, 0, 0, U_0 n_3, -U_0 n_2). \tag{2.17}$$

The complete radiation boundary value problem is represented by:

$$\begin{aligned}
\nabla^2\phi_k &= 0, && in \;\; V;\\
(\tfrac{\partial}{\partial t} - U_0\tfrac{\partial}{\partial z})^2\phi_k + g\tfrac{\partial\phi_k}{\partial z} &= 0, && on \;\; z = 0;\\
\tfrac{\partial\phi_k}{\partial n} &= n_k\dot{\zeta}_k + m_k\zeta_k, && on \;\; S_B;\\
\nabla\phi_k &\to 0, && as \;\; R_1 \to \infty, \;\; z = 0;\\
\nabla\phi_k &\to 0, && as \;\; z \to -\infty;\\
\phi_k = 0 \;\; \tfrac{\partial\phi_k}{\partial t} &= 0, && at \;\; t = 0.
\end{aligned} \tag{2.18}$$

This BVP is used to solve the velocity potential in each of the 6 degrees of freedom.

2.2 Boundary Integral Equation

There are two different approaches to solve the BVP that were discussed in Chapter 1, the Rankine Panel Method and the Green function Method. The Rankine panel method distributes sources on the free-surface as on the body surface and forces the boundary condition on the free-surface. The Green function method only distributes sources on the body surface, because the Green function automatically satisfies the linearized free-surface condition. In this work, the Green function Method is applied. The body is panelized and each panel has a source singularity located at the panel centroid. Liapis (1986) explains that these source strengths are determined by solving a Fredholm integral of the second kind on the body surface. It is known that the Green function satisfies three boundary conditions, on the free surface, the bottom boundary, and the conditions at infinity. A time-dependent Green function is required to solve the case considered for this study. Liapis (1986) states the most appropriate Green function for this boundary value problem must represent an impulsive source below the free surface. Wehausen and Laitone (1960) developed a Green function of this type for infinite water depth for a field point $P(x, y, z)$ and source point $Q(x', y', z')$. This problem uses the Green function in the form represented by Qiu (2001):

$$G(P, Q, t-\tau) = G_0(P, Q)\delta(t-\tau) + H(t-\tau)F(P, Q, t-\tau). \tag{2.19}$$

with a rankine source

$$G_0 = \frac{1}{r} - \frac{1}{r'}, \tag{2.20}$$

where $\delta(t-\tau)$ is the Dirac Delta function and $H(t-\tau)$ is the Heaviside unit step function, where F is known as the memory part of the Green function and mathematically

represented by:

$$F(P,Q,t-\tau) = -\frac{1}{2\pi}\int_0^\infty \sqrt{gk}\sin[\sqrt{gk}(t-\tau)]e^{k(z+z')}J_0(kR)dk, \tag{2.21}$$

with

$$r = \sqrt{(x-x')^2+(y-y')^2+(z-z')^2}, \tag{2.22}$$

$$r_1 = \sqrt{(x-x')^2+(y-y')^2+(z+z')^2}, \tag{2.23}$$

$$R = \sqrt{(x-x')^2+(y-y')^2}, \tag{2.24}$$

and J_0 is the Bessel function of the zeroth order. The Green function represents the potential at the field point $P(x,y,z)$ and at time t due to an impulsive source $Q(x',y',z')$ which is instantaneously created at time t and completely annihilated at time τ. Liapis (1986) demonstrates that this source acts like an underwater disturbance that creates a Cauchy-Poisson type wave system represented by the memory terms contained in $F(P,Q,t-\tau)$. Liapis (1986) shows that the Green function can be solved from the following systems of differential equations:

$$\begin{gathered}\nabla^2 G(P,Q,t-\tau) = -4\pi\delta(P-Q)\delta(t-\tau),\\ (\tfrac{\partial}{\partial t} - U\tfrac{\partial}{\partial x})^2 G(P,Q,t-\tau) + g\tfrac{\partial G(P,Q,t-\tau)}{\partial z} = 0, \quad on \quad z=0;\\ G(P,Q,t-\tau), \tfrac{\partial G(P,Q,t-\tau)}{\partial t} = 0, \quad for \quad t<0;\end{gathered} \tag{2.25}$$

with the boundary conditions set for the boundary value problem described in Chapter 2. Using these boundary conditions with the defined Green function, a boundary integral equation can be obtain by applying Green theorem (Equation 2.26) to the bounded volume V.

$$\int_V (\Phi\nabla^2 G - G\nabla^2\Phi)dV = \int_{S_b}\left\{\Phi\frac{\partial G}{\partial n_P} - G\frac{\partial \Phi}{\partial n_P}\right\}dS. \tag{2.26}$$

The above equation is valid for time independent problems. In order to describe the time domain we must integrate both sides of the equation from 0 to t with respect to τ coupled with the properties of $G(P,Q;t-\tau)$ and the fact that Φ satisfies the Laplace equation everywhere in the fluid domain. Liapis (1986) derived Equation 2.27 to mathematically describe the velocity potential at any time t and any place $P(x,y,z)$ in the fluid domain. Liapis (1986) showed that the contribution to ϕ from the surface integral over the free surface can be reduced to a line integral about the water line of the vessel and proves that the final result for ϕ at a point in the fluid domain (V) is expressed by:

$$\begin{aligned}\Phi(P;t) = &\int_0^t \int_{S_b} [\Phi(Q;t)\frac{\partial G(P,Q;t-\tau)}{\partial n_P} - G(P,Q;t-\tau)\frac{\partial \Phi(Q;t)}{\partial n_P}]d\tau dS \\ &-\frac{1}{g}\int_0^t \int_\Gamma U_0^2[G(P,Q;t-\tau)\frac{\partial \Phi(Q;\tau)}{\partial x'} - \Phi(Q;\tau)\frac{\partial G(P,Q;t-\tau)}{\partial x'}]d\tau dl \\ &+\frac{1}{g}\int_0^t \int_\Gamma U_0[G(P,Q;t-\tau)\frac{\partial \Phi(Q;\tau)}{\partial \tau} - \Phi(Q;\tau)\frac{\partial G(P,Q;t-\tau)}{\partial \tau}]d\tau dl.\end{aligned} \tag{2.27}$$

Details of this formulation can be found in Liapis (1986). Equation 2.27 can also be re-written in terms of source distribution. To do this, an interior flow is considered and subtracted from the equation.

$$\sigma(P;t) = \frac{\partial \phi_e(Q;\tau)}{\partial n_P} - \frac{\partial \phi_i(Q;\tau)}{\partial n_P}, \tag{2.28}$$

$$\phi_e = \phi_i. \tag{2.29}$$

With a source strength denoted as $\sigma(P;t)$ (Equation 2.28) and the assumption of Equation 2.29 ϕ can be represented in its standard format:

$$\begin{aligned}\phi(P,t) = &\int_0^t \int_{S_{\bar{B}}} G(P,Q,t-\tau)\sigma(Q,\tau)d\tau ds \\ &+\frac{U_0^2}{g}\int_0^t \int_\Gamma \sigma(Q,\tau)n_1 G(P,Q,t-\tau)d\tau dl.\end{aligned} \tag{2.30}$$

For the present case, an "indirect" method is used.

The indirect method initially solves the source distribution from the initial BVP with the problem dependent body boundary condition. Once the source distributions are obtained, the velocity potential can be computed using Equation 2.30. The integral equation for the source strength is obtained by differentiating Equation 2.30 with respect to the normal on the body surface and setting it equal to the boundary condition resulting in:

$$\begin{aligned}\frac{\partial\phi(P,t)}{\partial n_P} = &-\frac{\sigma(P,t)}{2} - \int_0^t \int_{S_B} \sigma(Q,\tau)\frac{\partial G(P,Q,t-\tau)}{\partial n_P}d\tau dS \\ &-\frac{U_0^2}{g}\int_0^t \int_\Gamma \sigma(Q,\tau)n_1\frac{\partial G(P,Q,t-\tau)}{\partial n_P}d\tau dl.\end{aligned} \tag{2.31}$$

This equation is used to solve for the source strength on each panel. After the velocity potential is obtained, the hydrodynamic force on the body can be calculated as described in the following section.

2.3 Hydrodynamic Force

To determine the hydrodynamic force over the body surface (S_b), the dynamic pressure must be determined. The unsteady pressure in the fluid domain (V) is defined by Bernoulli's equation:

$$\vec{P}(x,y,z) = -\rho\left(\frac{\partial\phi}{\partial t} + \frac{1}{2}\nabla\phi^2 + gz\right). \tag{2.32}$$

This equation can be linearized to Equation 2.33 using the Neumann-Kelvin Linearization:

$$\vec{P}(P,t) = -\rho\frac{\partial\phi}{\partial t} - \rho\vec{W}\cdot\nabla\phi. \tag{2.33}$$

The pressure is then integrated over S_B to determine the dynamic force equation:

$$F_j(t) = \int_{S_B} P(P,t)n_j dS = -\rho\int_{S_B}\frac{\partial\phi_k}{\partial t}n_j dS - \rho\int_{S_B}(\vec{W}\cdot\nabla\phi_k)n_j dS. \tag{2.34}$$

The second term in Equation 2.34 is difficult to evaluate due to the derivative of the potential. The theorem developed by Ogilvie and Tuck (1969) is useful because it is possible to eliminate the gradient simplifying the evaluation of the force yielding:

$$F_j(t) = -\rho\int_{S_B}\frac{\partial\phi}{\partial t}n_j dS + \rho\int_{S_B}\phi m_j dS + \rho\oint_{\Gamma}\phi n_j(\vec{l}X\vec{n})\cdot\vec{W}dl. \tag{2.35}$$

Liapis (1986) shows this force can then be broken into two components, $\dot{g}_{jk}(t)$ and $h_{jk}(t)$:

$$F_{jk}(t) = -\dot{g}_{jk}(t) - h_{jk}(t), \tag{2.36}$$

$$\dot{g}_{jk}(t) = \rho\int_{S_B}\phi_k n_j dS, \tag{2.37}$$

$$h_{jk}(t) = -\rho\int_{S_B}\phi_k m_j dS + \rho\oint_{\Gamma}\phi_k n_j(\vec{l}X\vec{n})\cdot\vec{W}dl. \tag{2.38}$$

Equations 2.36 to 2.38 are used to determine the response function.

Chapter 3

Impulse Response Function

The complete boundary value problem solution is represented by the sum of all six degrees of freedom ($k = 1, 2, \cdots, 6$). It is important to decompose the potential into six individual potentials, each representing a degree of freedom, in order to simplify the problem. Each potential function must satisfy the Laplace equation, the linear free-surface condition, the body boundary condition and the conditions at infinity. Each potential can be solved as an independent boundary value problem (2.18) defined in Chapter 2. Due to the linearity of the boundary value problem, it is possible to decompose the problem by modeling the object as a set of linear equations (linear system). This allows the problem to have a simple input, ship motion in each degree of freedom, returning a generalized hydrodynamic force. Cummins (1962) defined an impulse response function for each degree of freedom which completely characterizes any stable linear system. If the response to a unit impulse is known, then the systems response to an arbitrary force can be determined. This is valid due to the problem maintaining linearity. The method is then applied to find the hydrodynamic force due to an arbitrary motion. To define this impulse response function, we must consider that the ship velocity at t=0 jumps from 0 to 1 in the k^{th} degree. This velocity spike

is so instantaneous it can be considered impulsive and represented by $\dot{\eta}_k(t) = \delta(t)$. The velocity spike will cause a force on the body from the surrounding fluid, known as the impulse response function. Cummins (1962) and Ogilvie (1964) consider this impulse and modified the body boundary condition given by:

$$\frac{\partial \phi_k}{\partial n} = n_k \delta(t) + m_k H(t). \tag{3.1}$$

From this new body boundary condition, it can be seen that the problem can be decomposed into two parts, a impulsive ($\psi_k(P)\delta(t)$) part and a memory ($X_k(P)H(t)$) part due to the nature of both the Dirac Delta and Heaviside unit step functions. The velocity potential is mathematically shown as:

$$\phi_k = \psi_k(P)\delta(t) + X_k(P)H(t). \tag{3.2}$$

If the following is defined on the body boundary condition (S_B),

$$\begin{aligned} \frac{\partial \psi_k}{\partial n} &= n_k, \\ \frac{\partial X_k}{\partial n} &= m_k, \end{aligned} \tag{3.3}$$

then the new decomposed potentials will satisfy the body boundary conditions for all time. Due to the Dirac delta function, it is known that ψ_k potential describes the fluid motion for the impulsive stage and must satisfy the following boundary value problem:

$$\begin{aligned} \psi_k &= 0, \quad \text{on} \quad z = 0; \\ \frac{\partial \psi}{\partial n} &= n_k, \quad \text{on} \quad S_B; \\ \nabla \psi_k &\to 0, \quad \text{at} \quad \infty. \end{aligned} \tag{3.4}$$

The Heaviside unit step function characterizes $X_k(P)$ as the potential which represents the memory part (radiated waves) due to the impulse of the Dirac delta function. This potential can be further decomposed into two parts. The first representing the potential due to the change in body orientation as a result from the sudden velocity impulse. Due to the velocity jump from 0 to 1, the body will have a new position in the k^{th} degree of freedom. Since the problem deals with a steady flow field, this position change will cause a change in the fluid velocity on the body surface (S_B). These changes must be taken into account and removed from the equation to maintain the body boundary condition. Therefore ($\frac{\partial X_k}{\partial n}$) must be equal to m_k on the body surface for all time ($t > 0$). The second part represents the potential due to the disturbance in the flow field, which is a result of the velocity impulse. The disturbance in time radiates as a wave from the body. Therefore X_k must satisfy the following boundary value problem:

$$\begin{aligned} X_k &= 0, \qquad \text{on} \quad z = 0; \\ \frac{\partial X_k}{\partial t} &= -g\frac{\partial \psi_k}{\partial z}, \quad \text{on} \quad z = 0. \end{aligned} \tag{3.5}$$

Liapis (1986) attempted to improve computational efficiency by representing these two components of X_k explicitly in the following form:

$$X_k(P,t) = \varphi_k(P)H(t) + \bar{X}_k(P,t), \tag{3.6}$$

where φ_k represents the potential created from the change in body orientation during the impulsive velocity stage. The potential must satisfy the following boundary conditions:

$$\begin{aligned} \varphi_k &= 0, \quad \text{on} \quad z = 0; \\ \frac{\partial \varphi}{\partial n} &= m_k, \quad \text{on} \quad S_B; \\ \nabla\varphi_k &\to 0, \quad \text{at} \quad \infty. \end{aligned} \tag{3.7}$$

To maintain the original boundary conditions of X_k, $\bar{X}_k(P,t)$ must satisfy the following boundary conditions:

$$\begin{aligned}
\bar{X}_k &= 0, && \text{at } t=0;\\
\frac{\partial \bar{X}_k}{\partial t} &= -g\frac{\partial \psi_k}{\partial z}, && \text{on } z=0 \text{ at } t=0;\\
\frac{\partial \bar{X}_k}{\partial t} &= -g\frac{\partial \varphi_k}{\partial z}, && \text{on } z=0 \text{ at } t=0;\\
\frac{\partial \bar{X}_k}{\partial n} &= 0, && \text{on } z=0 \text{ for } t>0;\\
((\frac{\partial}{\partial t} - U_0^2\frac{\partial}{\partial x})^2 + g\frac{\partial}{\partial z})(\bar{X}_k + \varphi_k) &= 0, && \text{on } z=0 \text{ for } t>0.
\end{aligned} \tag{3.8}$$

The potential for the arbitrary forced motion in the k^{th} degree of freedom in terms of the non-impulse input velocity $\dot{\eta}k(t)$ can be found by integrating Equation 3.1 and evaluating the convolution of $\phi(P,t)$ with $\dot{\eta}k(t)$. The resulting potential is given by:

$$\phi_k = \int_{t_0}^{t} d\tau \phi_k(P,\tau)\dot{\eta}_k(\tau) = \psi_k(P)\dot{\eta}_k(t) + \varphi(P)\eta_k(t) + \int_{t_0}^{t} \bar{X}_k(P,\tau)\dot{\eta}_k(t-\tau)d\tau. \tag{3.9}$$

Cummins (1962) showed that $\phi_k(P,t)$, in its decomposed format, satisfies the body boundary condition, the free surface condition, and the conditions at infinity for all time. It is important to note that each potential, ψ_k, φ_k, and $\bar{X}_k$ must be solved from its individual boundary value problem Equations 3.4, 3.7, and 3.8, respectively. Substituting the new decomposed potential in the hydrodynamic force equation (Equation 2.35), causes the force equation to transform into Equation 3.10. This format has each component of the decomposed potential present in the following force evaluation:

$$F_{jk}(t) = -\mu_{jk}\ddot{\eta}_k(t) - b_{jk}\dot{\eta}_{jk}(t) - c_{jk}\eta_k(t) - \int_0^t d\tau K_{jk}(t-\tau)\dot{\eta}_{jk}(\tau), \tag{3.10}$$

where

$$\mu_{jk} = \rho \int_{s_B} \psi_k n_j dS,$$
$$b_{jk} = \rho[\int_{s_B} \varphi_k n_j dS - \int_{s_B} \psi_k m_j dS - \oint_\Gamma \psi_k n_j (\vec{l} X \vec{n}) \cdot \vec{W} dl],$$
$$c_{jk} = -\rho[\int_{s_B} \varphi_k m_j dS - \oint_\Gamma \varphi_k n_j (\vec{l} X \vec{n}) \cdot \vec{W} dl],$$
$$K^R_{jk}(t) = \rho[\int_{s_B} \frac{\partial \bar{X}_k}{\partial t} n_j dS - \int_{s_B} \bar{X}_k m_j dS - \oint_\Gamma \bar{X}_k n_j (\vec{l} X \vec{n}) \cdot \vec{W} dl].$$

μ_{jk}, is the time independent added mass of the floating body, that is only dependent on geometry. Both b_{jk} and c_{jk}, are coefficients that depend on geometry and forward speed, representing hydrodynamic damping and restoring force. The final term, $K^R_{jk}(t)$, represents the memory of the fluid due to the impulse velocity. It is also a function of geometry, speed, and time. It is important to note that μ_{jk} and b_{jk} are frequency independent parts of the added mass and damping. Liapis (1986) demonstrates that all frequency dependencies of the added mass and damping are contained in the memory function $K^R_{jk}(t)$. The impulse response function $K^R_{jk}(t)$ can be evaluated by using a non-impulsive input velocity defined in Equation 3.11. The purpose of this function is to remove the high frequency content of the impluse input, resulting in minimal numerical error.

$$\begin{aligned} \eta_k(t) &= \frac{1}{2}[1 + erf(\sqrt{\alpha t})], \\ \dot{\eta}_k(t) &= \sqrt{\tfrac{\alpha}{\pi}} e^{-\alpha t^2}, \\ \ddot{\eta}_k(t) &= -2\alpha t \dot{\eta}_k(t), \end{aligned} \tag{3.11}$$

where α is an arbitrary chosen constant that controls the frequency of the input. As $\alpha \rightarrow \infty$ the input function approaches the Dirac Delta function ($\delta(t)$). Applying this

function to the boundary value problem changes the body boundary condition to:

$$\frac{\partial \phi_k}{\partial n} = n_k \dot{\zeta}_k + m_k \zeta_k = n_k \dot{\eta}_k + m_k \eta_k. \tag{3.12}$$

Therefore the impulse response function can be determined from the following equation:

$$\int_0^t d\tau K_{jk}(t-\tau)\dot{\eta}_{jk}(\tau) = \dot{g}_{jk}(t) + h_{jk}(t) - \mu_{jk}\ddot{\eta}_k(t) - b_{jk}\dot{\eta}_{jk}(t) - c_{jk}\eta_k(t). \tag{3.13}$$

A benefit of the non-impulsive input is that it only requires a relatively small number of computational time steps to accurately determine the response function. Consequently, using Equation 3.13, the radiation force can be determined through the previously defined Equation 3.10.

3.1 Solving the Response Function

The method applied in this study is to solve for the hydrodynamic force (pressure) using Bernoulli's equation and then subtract the components from the force to obtain the response function $K_{jk}^R(t)$. The hydrodynamic force can mathematically represented by:

$$F_r(t) = \int_0^t K_{jk}^R(t)\dot{\eta}_k(t) \tag{3.14}$$

where:

$$F_r(t) = \dot{g}_{jk}(t) + h_{jk}(t) - \mu_{jk}\ddot{\eta}_k(t) - b_{jk}\dot{\eta}_{jk}(t) - c_{jk}\eta_k(t). \tag{3.15}$$

Cong et al (1998) showed that this function can be solved using a direct solution scheme as follows:

$$F_{r_m} = \sum_{n=1}^{m-1} K_{r_{m-n}} \eta_{I_n} \Delta t + \frac{1}{2}[K_{r_m} \eta_{I_0} + K_{r_0} \eta_{I_m}]\Delta t, \qquad m = 1, 2, \cdots, M, \tag{3.16}$$

where M is the total number of steps in time. Equation 3.16 is a set of equations that can be represented in the following matrix format:

$$\begin{bmatrix} \frac{1}{2}\eta_{I_1} K_{r_0} & + & \frac{1}{2}\eta_{I_0} K_{r_1} & & & & \\ \frac{1}{2}\eta_{I_2} K_{r_0} & + & \eta_{I_1} K_{r_1} & + & \frac{1}{2}\eta_{I_0} K_{r_2} & & \\ \cdots & & & & & & \\ \frac{1}{2}\eta_{I_M} K_{r_0} & + & \eta_{I_{M-1}} K_{r_1} & + & \cdots & + \eta_{I_1} K_{r_{M-1}} & + \frac{1}{2}\eta_{I_0} K_{r_M} \end{bmatrix} = \begin{bmatrix} \frac{F_{r_1}}{\Delta t} \\ \frac{F_{r_2}}{\Delta t} \\ \cdots \\ \frac{F_{r_M}}{\Delta t} \end{bmatrix}. \tag{3.17}$$

Chapter 4

Numerical Implementation

To properly implement the preceeding mathematical equations into a computer program, the equations must be represented in their discrete format. The following equations are discussed in the order in which they are solved within the program. The code was written in FORTRAN 90 using a Gaussian elimination solver to solve the system of equations.

4.1 Zero Forward Speed

The first special case is when the object has zero forward speed ($U_0 = 0$ and $m_j = 0$), thus allowing the removal of the line integration and changing the original source strength equation (Equation 2.30) into it's new format (Equation 4.1). The equation must be rearranged to move the unknown terms to the left hand side, while the known terms are on the right hand side, resulting in:

$$\frac{\partial \phi(P,t)}{\partial n_P} = -\frac{\sigma(P,t)}{2} + \int_{s_B}^{t} d\tau \int_{s_B} \sigma(Q,\tau) \frac{\partial G(P,Q,t-\tau)}{\partial n_P} dS, \tag{4.1}$$

$$V_n(P_i,t) = -\frac{\sigma(P,t)}{2} + \int_{S_B} \frac{\partial G_0(P,Q)}{\partial n_P}\sigma(Q,t)dS + \int_{t_0}^{t} d\tau \int_{S_B} \sigma(Q,\tau)\frac{\partial F(P,Q,t-\tau)}{\partial n_P}dS, \tag{4.2}$$

$$\int_{S_B} \frac{\partial G_o(P,Q)}{\partial n_P}\sigma(Q,t)ds = V_n(P_i,t) - \int_{S_B}\int_{t_o}^{t_{n-1}} d\tau \frac{\partial F(P,Q;t-\tau)}{\partial n_p}\sigma(P,\tau)ds, \tag{4.3}$$

where $V_n = \frac{\partial \phi}{\partial n_P}$, is the boundary condition $\dot{\eta} n_i$, it is important to note that the $-\frac{1}{4\pi}$ term is absorbed into the Green function. Equation 4.3 is represented in matrix form:

$$[B]_i = [H]_{ij}[\sigma(t_{kt})]_j, \tag{4.4}$$

with N representing the number of panels and kt is the current time step. The matrix terms are defined by:

$$H_{ii} = -0.5, \tag{4.5}$$

$$H_{ij} = -\int_{S_B} n_j \cdot \nabla(\frac{1}{r} - \frac{1}{r'}), \quad i \neq j; \tag{4.6}$$

$$B_i = V_n(P_i,t_{kt}) - \sum_{j=1}^{N}[\frac{\sigma(Q_j,t_{kt-1})}{2} \cdot \Delta t(\frac{\partial F(P_i,Q_j,t_{kt}-t_{kt-1})}{\partial n_{P_i}})] - \sum_{j=1}^{N}\sum_{k=1}^{kt-1}[\sigma(Q_j,t_k) \cdot \Delta t(\frac{\partial F(P_i,Q_j,t_k-t_{k-1})}{\partial n_{P_i}})]. \tag{4.7}$$

It can be seen that Equation 4.7 is independent of time. The "kernel" matrix does not change throughout the time domain simulation, meaning that the H matrix only needs to be inverted once at the beginning of the computation.

The velocity potential at time t on the body surface is derived through the following equations:

$$\phi(P,t) = \int_{t_0}^{t} d\tau \int_{S_B} G(P,Q,t-\tau)\sigma(Q,\tau)ds, \tag{4.8}$$

$$\begin{aligned}\phi(P,t) &= \int_{S_{\bar{B}}} G_0(P,Q)\sigma(Q,t)ds \\ &+ \sum_{k=1}^{kt}[\int_{S_B} \sigma(Q,t_k)\cdot\Delta t(F(P,Q,t_k-t_{k-1}))]ds.\end{aligned} \tag{4.9}$$

The final discrete format is given by:

$$\begin{aligned}\phi(P,t) &= \sum_{n=1}^{N} G_0(P,Q)\sigma(Q,t) \\ &+ \sum_{n=1}^{N}\sum_{k=1}^{kt}[\sigma(Q,t_k)\cdot\Delta t(F(P,Q,t_k-t_{k-1}))].\end{aligned} \tag{4.10}$$

4.2 Non-Zero Forward Speed

For the case when there is a forward speed, the line integral and m-terms must be included. Equation 2.31 expands to the following:

$$\begin{aligned}\frac{\partial\phi(P,t)}{\partial n_P} &= -\frac{\sigma(P,t)}{2} - \int_{S_{\bar{B}}} \sigma(Q,t)\frac{\partial G_0(P,Q)}{\partial n_P}dS \\ &- \int_o^t d\tau \int_{S_{\bar{B}}} \sigma(Q,\tau)\frac{\partial F(P,Q,t-\tau)}{\partial n_P}dS \\ &- \frac{U_0^2}{g}\int_\Gamma \sigma(Q,t)n_1\frac{\partial G_0(P,Q)}{\partial n_P}dl \\ &- \frac{U_0^2}{g}\int_0^t d\tau \int_\Gamma \sigma(Q,\tau)n_1\frac{\partial F(P,Q,t-\tau)}{\partial n_P}dl,\end{aligned} \tag{4.11}$$

$$\begin{aligned}&\frac{\partial\phi(P,t_{kt})}{\partial n_P} + \Delta t\sum_{k=1}^{kt}\int_{S_{\bar{B}}} \sigma(Q,t_k)\frac{\partial F(P,Q,t-t_k)}{\partial n_P}dS \\ &+\Delta t\frac{U_0^2}{g}\sum_{k=1}^{kt}\int_\Gamma \sigma(Q,t_k)n_1\frac{\partial F(P,Q,t-t_k)}{\partial n_P}dL \\ &= -\frac{\sigma(P,t)}{2} + \int_{S_{\bar{B}}} \sigma(Q,t_{kt})\frac{\partial G_0(P,Q)}{\partial n_P}dS \\ &- \frac{U_0^2}{g}\int_\Gamma \sigma(Q,t_{kt})n_1\frac{\partial G_0(P,Q)}{\partial n_P}dl.\end{aligned} \tag{4.12}$$

Note that the time summations in Equation 4.12 require half weights at the end points due to the use of a trapezoidal integration rule. Transforming Equation 4.12 into:

$$
\begin{aligned}
&\frac{\partial\phi(P,t_{kt})}{\partial n_P}+\frac{\Delta t}{2}\int_{\bar{S_B}}\sigma(Q,t_{kt})\frac{\partial F(P,Q,0)}{\partial n_P}ds\\
&+\frac{\Delta t U_0^2}{2g}\int_{\Gamma}\sigma(Q,t_{kt})n_1\frac{\partial F(P,Q,0)}{\partial n_P}dL\\
&+\Delta t\sum_{k=1}^{kt-1}\int_{\bar{S_B}}\sigma(Q,t_k)\frac{\partial F(P,Q,t_{kt}-t_k)}{\partial n_P}ds\\
&+\Delta t\frac{U_0^2}{g}\sum_{k=1}^{kt-1}\int_{\Gamma}\sigma(Q,t_k)n_1\frac{\partial F(P,Q,t_{kt}-t_k)}{\partial n_P}dL\\
&=-\frac{\sigma(P,t)}{2}+\int_{S_{\bar{B}}}\sigma(Q,t_{kt})\frac{\partial G_0(P,Q)}{\partial n_P}dS\\
&-\frac{U_0^2}{g}\int_{\Gamma}\sigma(Q,t_{kt})n_1\frac{\partial G_0(P,Q)}{\partial n_P}dl,
\end{aligned}
\tag{4.13}
$$

making use of the conditions:

$$
\begin{aligned}
F(P,Q,0)&=0,\\
\frac{\partial F(P,Q,0)}{\partial n_P}&=0,
\end{aligned}
$$

Equation 4.13 becomes:

$$
\begin{aligned}
&\frac{\partial\phi(P,t_{kt})}{\partial n_P}+\Delta t\sum_{k=1}^{kt-1}\int_{\bar{S_B}}\sigma(Q,t_k)\frac{\partial F(P,Q,t_{kt}-t_k)}{\partial n_P}ds\\
&+\Delta t\frac{U_0^2}{g}\sum_{k=1}^{kt-1}\int_{\Gamma}\sigma(Q,t_k)n_1\frac{\partial F(P,Q,t_{kt}-t_k)}{\partial n_P}dL\\
&=-\frac{\sigma(P,t)}{2}+\int_{S_{\bar{B}}}\sigma(Q,t_{kt})\frac{\partial G_0(P,Q)}{\partial n_P}dS\\
&-\frac{U_0^2}{g}\int_{\Gamma}\sigma(Q,t_{kt})n_1\frac{\partial G_0(P,Q)}{\partial n_P}dl.
\end{aligned}
\tag{4.14}
$$

As with the zero forward speed case, the equation can be represented in matrix form:

$$
[B]_i=[H]_{ij}[\sigma(t_{kt})]_j, \tag{4.15}
$$

where kt stands for the current time step, N represents the panel number. The matrix terms are defined by:

$$H_{ii} = -0.5 - \frac{U_0^2}{g}\int_{\Gamma_j} n_i \cdot \nabla(\frac{1}{r} - \frac{1}{r'})dL, \tag{4.16}$$

$$\begin{aligned} H_{ij} = &-\int_{S_B} n_i \cdot \nabla(\frac{1}{r} - \frac{1}{r'}) \\ &-\frac{U_0^2}{g}\int_{\Gamma_j} n_i \cdot \nabla(\frac{1}{r} - \frac{1}{r'})dL, \quad i \neq j; \end{aligned} \tag{4.17}$$

$$\begin{aligned} B_i = &\sum_{n=1}^{N}(\frac{\partial\phi(P_i, t_{kt})}{\partial n_{P_i}} \\ &+\Delta t\sum_{k=1}^{kt-1}\int_{S_{\bar{B}}} \sigma(Q_j, t_k)\frac{\partial F(P_i, Q_j, t_{kt} - t_k)}{\partial n_{P_i}}) \\ &+\sum_{j^*}\Delta t\sum_{k=1}^{kt-1}\frac{U_0^2}{g}\int_{\Gamma_{j^*}} \sigma(Q_{j^*}, t_k)\frac{\partial F(P_i, Q_{j^*}, t_{kt} - t_k)}{\partial n_{P_i}}dL, \end{aligned} \tag{4.18}$$

where j^* means that only the panels on the free surface are used for the summation of the line integrals. The source strength for the line integral segment is assumed to be the same as the source strength of the panel directly below it. As with the no-forward speed case, the $[H]_{ij}$ matrix is independent of time, so only one inversion is required for all time domain computations. It is also important to note that the line integration part of the "Rankine Source" is zero, due to the fact at the free surface $\frac{1}{r} - \frac{1}{r'} = 0$. After the solution for the source strengths over all panels are determined for every time step, the velocity potential can be determined through Equation 2.30.

The final discrete form is given by:

$$\begin{aligned}\phi(P_i,t) = \frac{\sigma(P_i,t)}{2} &+ \sum_{j=1}^{N}\int_{S_{\bar{B}}} G_0(P_i,Q_j)\sigma(Q_j,t)dS \\ &+\frac{U_0^2}{g}\sum_{j^*=1}^{N}\int_{\Gamma} G_0(P_i,Q_j)\sigma(Q_j,t)dL \\ \Delta t\sum_{k=1}^{kt}\sum_{j=1}^{N}&\int_{S_{\bar{B}}} F(P_i,Q_j,t_{kt}-t_k)\sigma(Q_j,t_k)dS \\ +\frac{U_0^2}{g}\Delta t\sum_{k=1}^{kt}\sum_{j^*=1}^{N}&\int_{S_\Gamma} F(P_i,Q_j,t_{kt}-t_k)\sigma(Q_j,t_k)dL.\end{aligned} \tag{4.19}$$

Chapter 5

Numerical Results

The following section presents the validation of the radiation problems for a Hemisphere and Wigley Hull. The zero speed and forward speed radiation problems were applied to the Wigley Hull, while only the zero speed case was applied to the Hemisphere.

5.1 Hemisphere

The first set of validations were performed on a hemisphere. The panelization was only over half the hemisphere due to symmetry about the x-axis.

Due to the importance of the $\frac{1}{r} - \frac{1}{r'}$ term to the entirety of the numerical scheme it is important to verify this before applying it to the time-domain integration. This is verified by computing the time-independent heave added-mass of a floating hemisphere at the short wave limit. Newman (1977) determined that this added-mass can be computed using the $\frac{1}{r} - \frac{1}{r'}$, while Havelock (1955) presented a non-dimensional analytical solution of 0.5. The present code produced a non dimensional result of 0.526 with 100 panels and 0.518 with 225 panels. These results are reasonable when compared with the panel method SEALOADS that produced a non-dimensional result

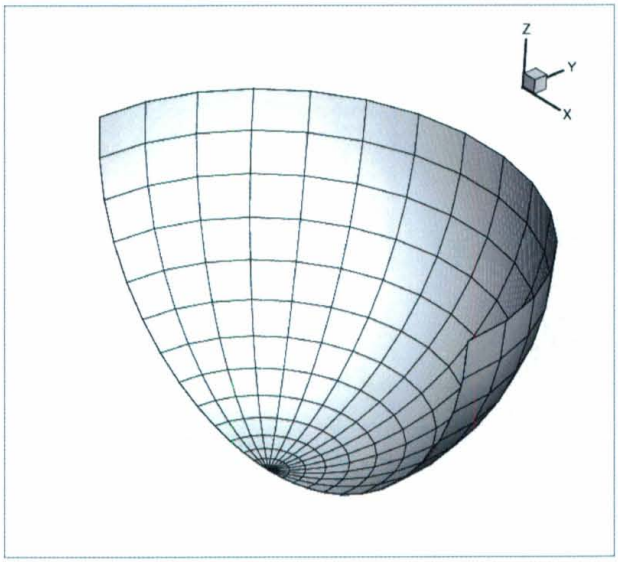

Figure 5.1: Hemisphere Mesh for 225 Panels

of 0.517 with 256 flat panels over a hemisphere (Qiu, 2001).

The developed panel method was used to compute the radiation heave response function for a hemisphere of radius of 5 meters. The response function was non-dimensionalized by:

$$\frac{K_{33}}{\rho \nabla \sqrt{\frac{R}{g}}}, \tag{5.1}$$

while time was non-dimensionalized by:

$$t\sqrt{\frac{g}{R}}, \tag{5.2}$$

where R is the radius of the hemisphere, g is acceleration due to gravity ($9.81\ \frac{m}{s^2}$), and ∇ is the hemisphere volume of displacement. The chosen time step, Δt was 0.05 seconds. Figure 5.2 shows that the response function agreed with results from Qiu (2001) and the analytical solution produced by Barakat (1962).

The code uses the computed response function to compute the added-mass (A_{33})

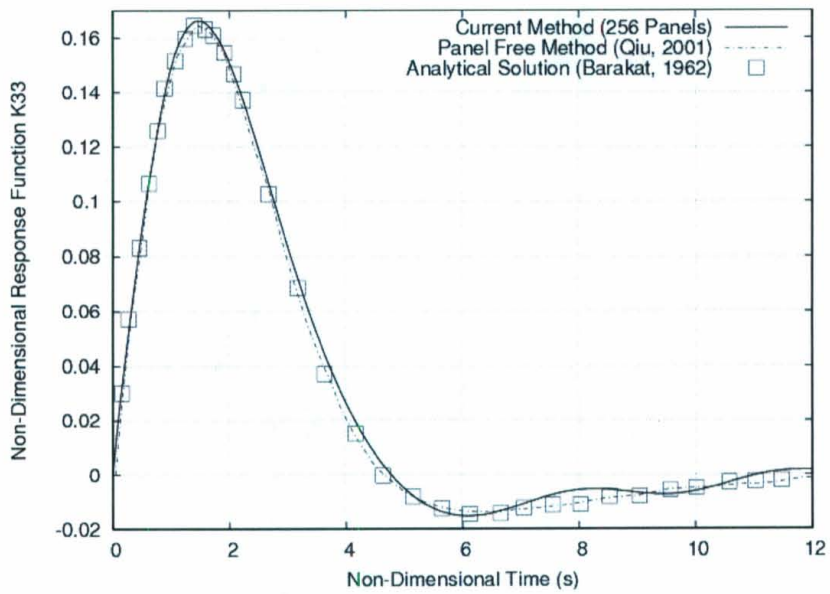

Figure 5.2: Non-dimensional Heave Response Function Versus Non-dimensional Time

and damping coefficients (B_{33}) of a heaving hemisphere versus non dimensional frequency. The added mass and damping coefficients are directly related to the cosine and sine transformation of the computed response function. The mathematical formulations that were used are:

$$A(\omega)_{jk} = \mu_{jk} - \frac{1}{\omega}\int_0^\infty K(t)_{jk}\sin(\omega t)dt, \tag{5.3}$$

$$B(\omega)_{jk} = b_{jk} - \int_0^\infty K(t)_{jk}cos(\omega t)dt, \tag{5.4}$$

where μ_{jk} and b_{jk} are the time-independent parts of the added-mass and damping coefficients. The frequency was non-dimensionalized by:

$$\omega^2\frac{R}{g}, \tag{5.5}$$

while the added-mass and damping coefficients were non-dimensionalized by:

$$\frac{A_{33}}{\frac{2}{3}\rho\phi R^3}, \tag{5.6}$$

$$\frac{B_{33}}{\frac{2}{3}\rho\phi R^3}. \tag{5.7}$$

The results were compared to analytical results produced by Hulme (1982). Figures 5.3 and 5.4 show reasonable agreement. Hulme (1982) showed that an irregular frequency response occurs at:

$$\omega_{irr}^2 \frac{a}{g} \approx 2.56. \tag{5.8}$$

It can be seen from the graph that at a low panelization we seen a similar phenomena reported by Lin & Yue (1991). This was referred to a solution oscillation at an irregular frequency behavior near ω_{irr}. However when the panel number is increased this irregularity begins to disappear.

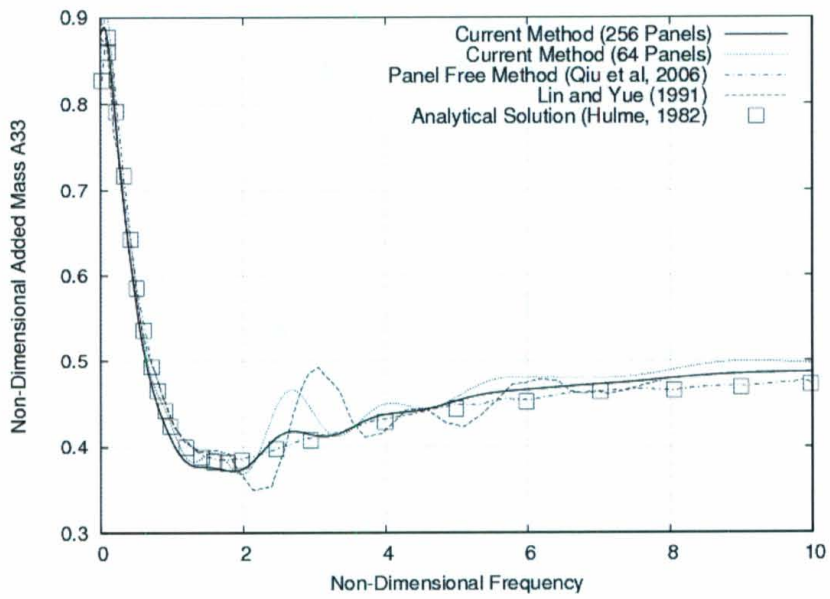

Figure 5.3: Non-dimensional Heave Added Mass Versus Non-dimensional Frequency

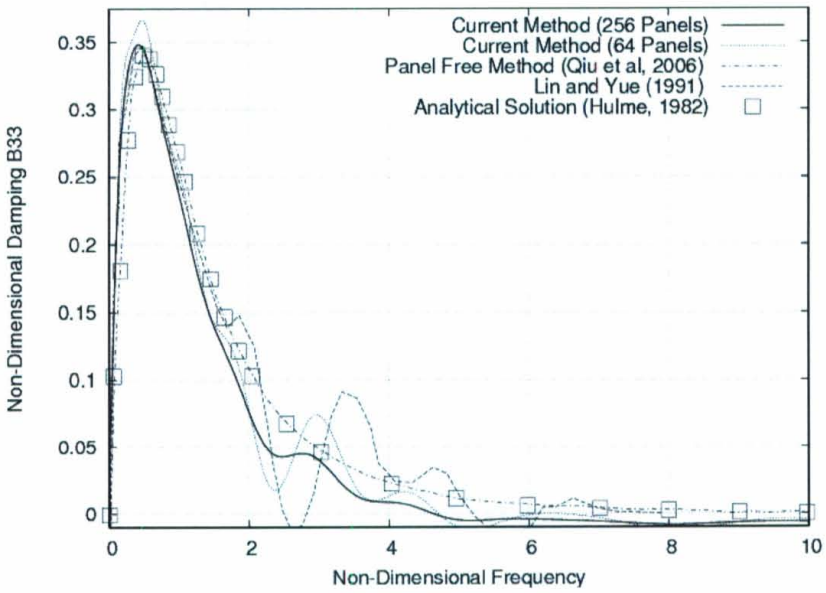

Figure 5.4: Non-dimensional Heave Damping Versus Non-dimensional Frequency

5.1.1 Single Source Point

Before computing the forward speed cases of the Wigley Hull, it was important to verify the Green function ability to compute the forward speed case. The code was applied to a single moving source point at a constant source strength to validate the wave pattern. Due to the Kelvin-Neumann linearization, a "Kelvin" wave pattern is to be expected. Figure 5.5 illustrates this particular type of a wave pattern.

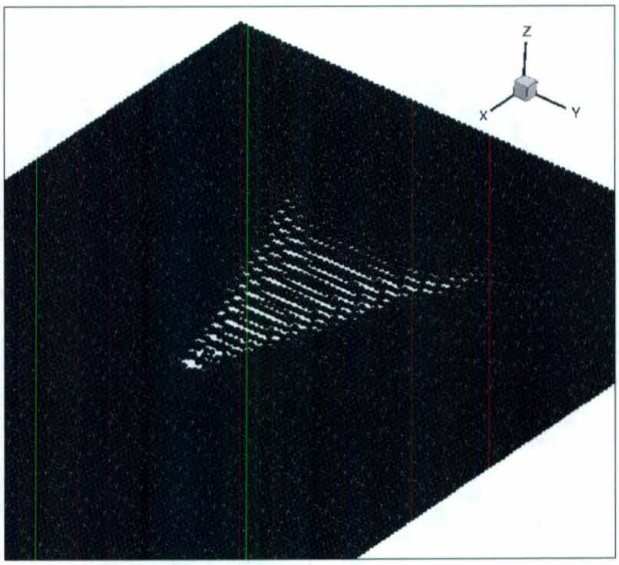

Figure 5.5: Single Moving Source Points with Constant Source Strength

5.2 Wigley Hull

5.2.1 Zero Forward Speed

The developed panel method has been applied to the Wigley Hull at zero forward speed and non-zero forward speed cases. The Wigley Hull geometry is defined by (Journee, 1992) :

$$\eta = (1-\zeta^2)(1-\xi^2)(1+\beta\xi^2) + \alpha\zeta^2(1-\zeta^8)(1-\xi^2)^4, \tag{5.9}$$

where;

- $\alpha = 1.0$ and $\beta = 0.2$ for models W_I and W_{II}
- $\alpha = 0$ and $\beta = 0.2$ for models W_{III} and W_{IV}
- $\alpha = 0$ and $\beta = 0$ for model W_{RT}

Qiu (2001) defines the non-dimensional variables by:

$$\eta = \frac{2y}{B}, \quad \xi = \frac{2x}{L}, \quad \zeta = \frac{z}{T}, \tag{5.10}$$

where L is the ships length, B is the beam, and T is the draft. Length and beam are taken at the water line. Figure 5.6 shows the mesh of W_I with 256 panels over the half body.

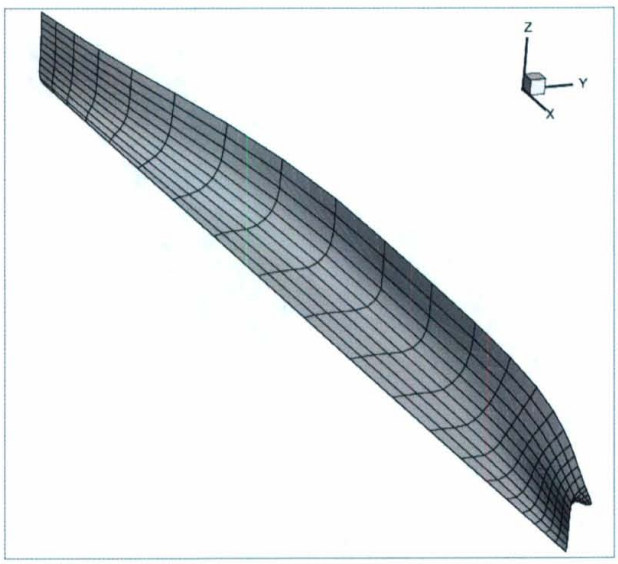

Figure 5.6: Wigley Hull W_I Mesh for 256 Panels

The Wigley Hull W_I was used to validate the heave response function Figure 5.7 and pitch response function Figure 5.8. The hull used had a block coefficient (C_b) of 0.5606 with the dimensions given by (Qiu, 2001):

$$\frac{B}{L} = 0.10, \quad \frac{T}{L} = 0.0625, \quad L = 120.0. \tag{5.11}$$

The response functions were found to be quite sensitive to the number of panels along the z-direction, while the chosen number of panels along the x-direction

have minimal effect. This is due to the properties of the Green function and its sensitivity when the centroid of a panel approaches the free surface, see Section 5.3 for further discussion. The response function for heave (K_{33}) and pitch (K_{55}) were non-dimensionalized by:

$$\frac{K_{33}}{\frac{\rho g \nabla}{L}}\sqrt{\frac{g}{L}}, \tag{5.12}$$

$$\frac{K_{55}}{\rho g \nabla}\sqrt{\frac{g}{L}}, \tag{5.13}$$

and time was non-dimensionalized by:

$$t\sqrt{\frac{g}{L}}. \tag{5.14}$$

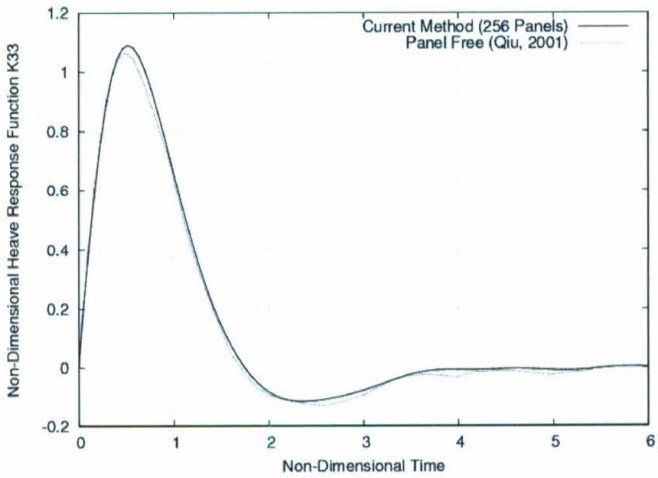

Figure 5.7: Wigley Hull W_I Heave Response Function K33

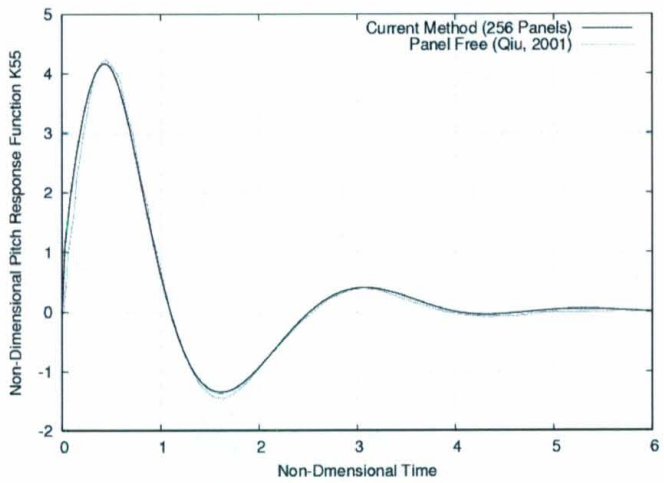

Figure 5.8: Wigley Hull W_I Pitch Response Function K55

The zero speed heave coefficients of added-mass and damping for the Wigley Hull were computed from their respective response functions. The frequency was non-dimensionalized by:

$$\omega_{ND} = \sqrt{\omega \frac{g}{L}} \tag{5.15}$$

The coefficients for heave added-mass (A_{33}) and damping (B_{33}) were non-dimensionalized by:

$$\frac{A_{33}}{\rho \nabla}, \tag{5.16}$$

$$\frac{B_{33}}{\rho \nabla \omega}. \tag{5.17}$$

The non-dimensional coefficients were compared to that of MIT's code TiMIT taken from Qiu (2001). The results shown in Figures 5.9 and 5.10 show reasonable agreement.

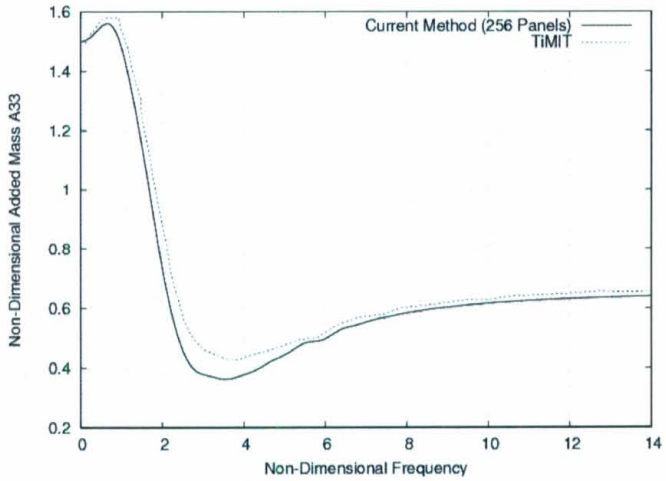

Figure 5.9: Wigley Hull W_I Non-dimensional Heave Added Mass Versus Non-dimensional Frequency

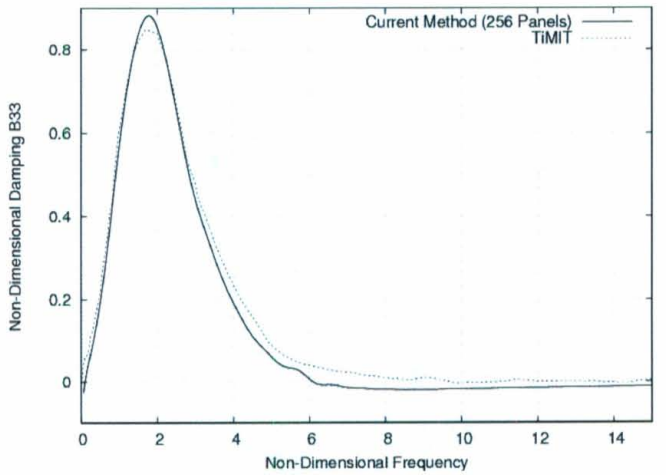

Figure 5.10: Wigley Hull W_I Non-dimensional Heave Damping Versus Non-dimensional Frequency

5.2.2 Non-Zero Forward Speed

When introducing forward speed into the computation, it increases the complexity of the computations. In this study, only the wave resistance problem is computed

in the forward speed problem. The Wigley Hull W_{RT} was used in the forward speed computation case. A number of Froude numbers were tested for the W_{RT} and the results were compared to experimental and numerical results. A key component to note is that with the forward speed case and the Green function, it is sensitive to the panel selection along the z-axis and the x-axis. It is important to select a sufficient number of panels along the x-direction to capture the wave along the body, while an incorrectly chosen number of panels in the z-axis can have a undesirable outcome. If the number of panels are too large or too few, the program will incorrectly predict the wave resistance. This is further discussed in Section 5.3.

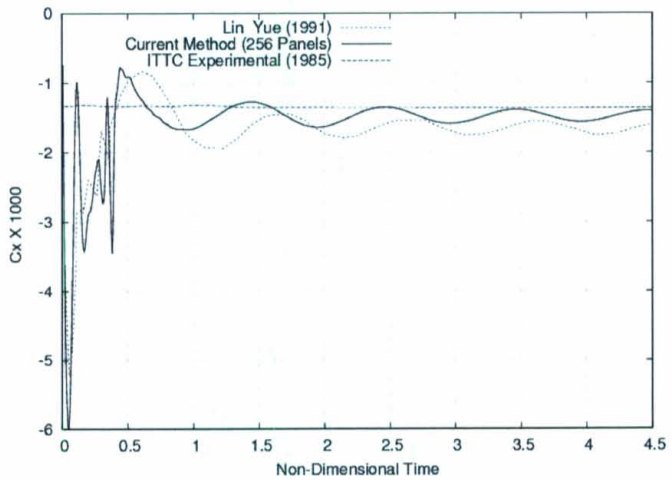

Figure 5.11: Surge Force (Wave Resistance) Wigley Hull W_{RT} for Fn=0.3

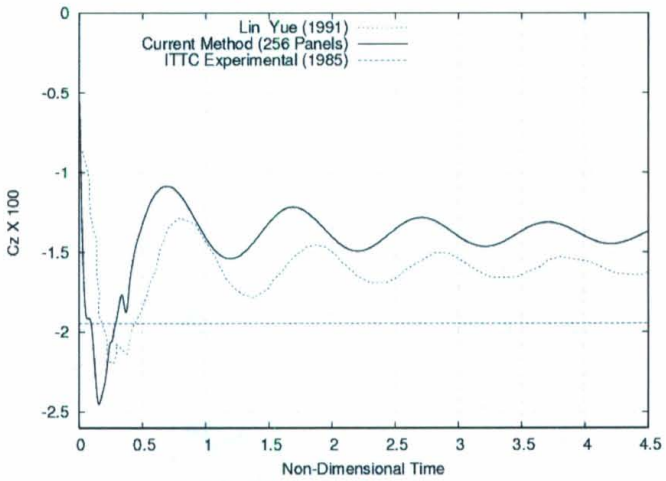

Figure 5.12: Heave Force Wigley Hull W_{RT} for Fn=0.3

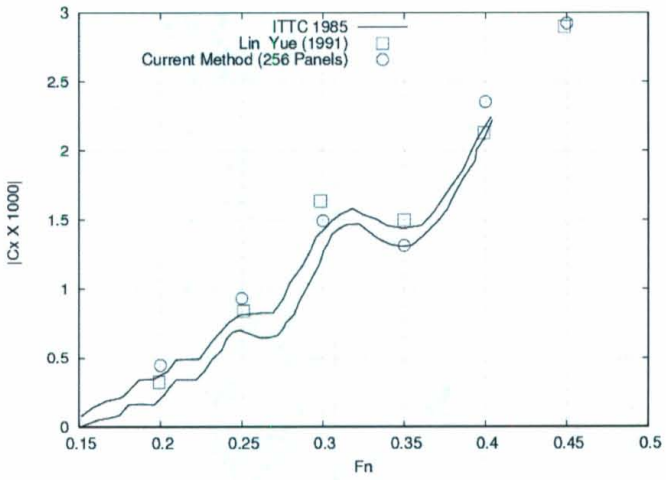

Figure 5.13: Wigley Hull W_{RT} Wave Resistance Versus Fn

The surge force (wave resistance) and vertical force were non-dimensionalized by:

$$C_i = \frac{F_i}{\frac{1}{2}\rho U^2 S}. \tag{5.18}$$

Time was non-dimensionalized by the oscillation period given by:

$$T_0 = T\frac{g}{8\pi U} \tag{5.19}$$

Figures 5.11 and 5.12 show the force results for constant forward speed at a Froude number of 0.3. Forces in the heave and surge direction were computed. The surge and heave forces are compared to Lin & Yue (1991) and the experimental results from ITTC, 1985. The present results agree with Lin & Yue and are reasonably close to the experimental results. To complete the wave resistance curve the program was run for a wide range of Froude numbers from 0.2 to 0.45 and compared again to the ITTC 1985 experimental result and Lin & Yue's results. Figure 5.13 represents the final wave resistance curve. From this curve it can be seen that there is reasonable agreement with the experimental and numerical results.

5.3 Discussion on Numerical Stability

During the progress of creating this numerical method to solve the ship resistance boundary value problem, many situations were encountered when dealing with the numerical stability of the program. The Green function as mentioned above plays a key role in the computations of this boundary value problem. It satisfies the conditions at infinity, bottom boundary, and the linear free surface. However, there are a number of things that must be considered when using the Green function. When panelizing an object, it is very important to create a cosine distribution of panels along the z-axis. This is due to the fact that Green function is highly oscillatory at the free surface. If an even panel distribution is used, unstable oscillations will occur, rendering inaccurate results. Thus it is imporant to maintain a relatively large panel size near the free surface.

When computing forward speed problems, the panelization along the z-axis and the x-axis is also important. If the z-direction has too many panels, even with a cosine distribution, the centroids of the panels will approach the free surface boundary, and if the centroid comes close enough to the free surface, large oscillations will occur. However, if the panelization is too low along the z-direction, the method will be unable to capture the entirety of the problem, also rendering inaccurate results. This can be a major problem when attempting to compute a solution for small objects. For example a ship model with a draft of 0.1875, would cause an issue. For panelization along the x-direction, is important for the panels to be able to capture the waves along the moving body. Should the panel number be low, the numerical method will be unable to capture the effects, producing in inaccurate results.

Chapter 6

Conclusions and Recommendations

A panel method computer program has been developed to solve the radiation problems in the time domain. This was done as the first step in creating a complete numerical model of the ship-ice interaction scenario. The validity of the approach and its accuracy were assessed by comparing results from the code with results from similar codes presented by Qiu (2001) and Lin & Yue (1991) for different geometries. The validation cases covered were the radiation problems, the computing of the coefficients of added-mass and damping along with the forward wave resistance. The present results are reasonable when compared to published results, both numerical and experimental.

6.1 Panelization

Numerical stability was fully investigated using the solution to the preceding defined boundary value problem. It was discovered that a stable solution for the Green function is dependent on the number and arrangement of the panels in the x and z directions. A cosine arrangement is required in order to avoid free surface oscillations. An excessive number of panels along the z direction can also produce large oscillations

in the solution, even with a cosine arrangement, due to the panel centroids being to close to the free surface. Choosing a panelization grid of 6 to 8 panels along the z-axis for the Wigley hull should minimize the errors. The optimal number of panels is beyond the scope of the current study, but it is expected that this may change with the size and geometry of the model. It is recommended that further research be preformed to find the optimum grid for a wide variety of geometries and speeds.

The main limitation of this method is the numerical manipulation that is required due to the assumption of having a constant source strength across each panel. This limits the ability for more accurate solutions. Another area of the code that required considerable effort was the line integration. This integration is preformed where the body intersects the free surface increasing the complexity of the integration. In the present study the integration assumes that the source strength at the free surface is equal to the source strength on the panel directly below the point on the line. It is recommended that the method to solve this integration be imporved, to increase accuracy.

6.2 Recommendations for Future Work

The Green function was a suitable choice for the present work. However, the Green function only satisfies the linear free surface condition. It is recommended that alternative methods be explored to implement a nonlinear free surface condition. One alternative may be the use of Rankine Source method. This method distributes sources on the free surface and forces the free surface boundary condition. This removes the Green function from the boundary value problem and allows for the possibility of non-linear free surface condition. Significant work has been done with this method and is quite mature.

Another approach may be to adopt a 'Panel Free' approach (Qiu & Hsiung, 2000) that is more robust and accurate than the present panel method. The method removes the singularity from the boundary value problem by the desingularization of the boundary integral equation. This allows the geometry of the body surface is be represented by Non-Uniform Rational B-Splines (NURBS) instead of panels. The integral equation can then be applied to the body by Gaussian quadrature, removing the issue of panelization. The method has minimal numerical manipulation, due to the removal of panels. Panel free has been proven to be more accurate since the body is described mathematically by NURBS as opposed to panels.

References

Aanesland, V. (1986). A three-dimensional panel method for calculating wave-making resitance. Trondheim, Norway.

Barakat, R. (1962). Vertical motion of a floating sphere in a sinewave sea. Journal of Fluid Mechanics, 13, 540-556.

Beck, R. & Magee, A. (1990). Time-domain analysis for predicting ship motions. Proceedings IUTAM symposium Dynamics of Marine Vehicles and Structures in Waves, London.

Beck, R. F. (1994). Time-domain computations for floating bodies. Applied Ocean Research, 16, 267-282.

Broeze, J., Daalen, E. F. G. van & Zandbergen, P. J. (1993). A three-dimensional panel method for nonlinear free surface waves on vector computers. Journal of Computational Mechanics, 13, 12-28.

Chang, M. (1977). Computation of three-dimensional ship-motions with forward speed. In Proceedings second international conference on numerical ship hydrodynamics (p. 124-135).

Clement, A. (1998). Computation of impulse response function using dierential properites of the time-domain green function. 13th International Workshop on Water Waves and Floating Bodies.

Cong, L., Huang, Z., Ando, S. & Hsiung, C. (1998). Time-domain analysis of ship motions and hydrodynamic pressures on a ship hull in waves. In 2nd interational conference on hydroelasticity in marine technology.

Cummins, W. E. (1962). The impulse response function and ship motions. Hydrome- chanics Laboratory Research and Development Report.

Dawson, C. (1977). A practical computer method for solcing ship-wave problems. In 2nd interational conference on numerical ship hydrodynamics.

Finkelstein, A. (1957). The initial value problem for transient water waves. Communications on Pure and Applied Mathematics, 10, 511-522.

Havelock, T. (1955). Waves due to a floating sphere making periodic heaving oscillations. In Proceedings of the rotal society (p. 1-7).

Hess, J. L. & Smith, A. M. O. (1964). Calculation of nonlifting potential ow about arbitrary three-dimensional bodies. Journal of Ship Research, 8 (3), 22-44.

Huang, Y. & Sclavounos, P. D. (1997). Nonlinear ship wave simulations by a rankine panel method. 12th International Workshop on Water Waves and Floating Bodies.

Hulme, A. (1982). The wave forces acting on a floating hemisphere undergoing forced periodic oscillations. Journal of Fluid Mech., 121, 443-463.

Inglis, R. & Price, W. (1982). A three-dimensional ship motion theory comparison between theoretical prediction and experimental data of hydrodynamic coeffcient with forward speed. Transaction Royal Insitution of Naval Architecture, 124, 141-157.

John, F. (1950). On the motion of floating bodies, ii. Communications in Pure and Applied Mathmatics, 3, 45-101.

Journee, J. (1992). Experiments and calculations on 4 wigley hull forms in head waves (Tech. Rep.). Delft University of Technology.

Kim, Y., Kim, K.-H., Kim, J.-H., Kim, T., Seo, M.-G. & Kim, Y. (2011). Time domain analysis of nonlienar motion response and structural loads on ships and offshore structures: Development of wish programs. Inter. JNav. Archit. Ocean Engineering, 3, 37-52.

Kim, Y.-H., Kim, S. H. & Lucas, T. (19o98). Advance panel method for ship wave inviscid ow theory (swift). Ship Hydromechanics Department research and Development Report.

King, B. K. (1987). Time-domain analysis of wave exciting forces on ships and bodies. Ph.D. Thesis, The University of Michigan.

Korsmeyer, F., Lee, C., Newman, J. & Sckavounos, P. (1988). The analysis of waves effects on tension-leg platforms. In Proceedings of 7th international conference on offshore mechanics and arctic engineering, houston. tx (p.

1-12).

Larsson, L. (1987). Numerical predictions of the ow and resistance components of sailing yachts. In Proceedings conference yachting technology., u.w. australia (p. 124-135).

Lee, C.-H., Maniar, H., Newman, J. & Zhu. X. (1997). Computations of Wave Loads Using a B-Spline Panel Method. Twenty-First Symposium on Naval Hydrodynamics. (p. 75-92).

Liapis, S. J. (1986). Time-domain analysis of ship motions. Ph.D. Thesis, The University of Michigan.

Lin, W. & Yue, D. (1991). Numerical solutions for large-amplitude ship motions in the time domain. 8th Symposium on Naval Hydrdodynamics, 41-66.

Michell, J. (1898). The wave resistance of a ship. Phil. Mag., 45, 106-123.

Nakos, D. & Sclavounos, P. (1990). Ships motions by a three-dimensional rankine panel method. 18th Symposium on Naval Hydrodynamics., Ann Arbor. Michigan.

Newman, J. (1977). Marine hydrodynamics. The MIT Press.

Newman, J. (1979). The theory of ship motions. Advances in Applied Mechanics, 18, 222-283.

Newman, J. (1985). Transient axisymmetric motion of a floating cylinder. Journal of Fluid Mechanics.

Ogilvie, T. F. (1964). Recent progress toward the understanding and prediction of ship motions. In Proceedings 5th symposium on naval hydrodynamics (p. 3-128).

Ogilvie, T. F. & Tuck, E. O. (1969). A rational strip theory of ship motion: Part i. (Tech. Rep. No. 13). The University of Michigan.

Qiu, W. & Peng, H. (2007). Computation of Large-Amplitude ship Motions in the Time Domain. 9th International Conference on Numerical Ship

Hydrodynamics, Ann Arbor, Michigan.

Qiu, W., Peng, H. & Chuang, J. (2006). Computation of Wave-body Interactions using the Panel-Free Method and Exact Geometry. Journal of Ocean Engineering, 29, 1555-1567

Qiu, W. (2001). A Panel-Free Method for Time-Domain Analysis of Floating Bodies in Waves. Ph.D Thesis, Dalhousie University.

Qiu, W. & Hsiung, C. C. (2000). A panel-free method for time-domain analysis of radiation problem. Journal of Ocean Engineering, 29, 1555-1567.

Savitsky, D. (2003). On the subject of high-speed monohulls. Of the Society Of Naval Architects and Marine Engineers.

Song, S. (1993). Computer simulation of ship waves. Ph.D Thesis, Memorial University of Newfoundland.

Stoker, J. (1957). Water waves. Pure and Applied Mathematics, 3.

Tuck, E. O. (1964). A systematic asymtotic expansion procedure for slender ships. Jounral of Ship Research, 8 (1), 15-23.

Wehausen, J. (1971). The motion of floating bodies. Annual Review of Fluid Mechanics, 3, 237-268.

Wehausen, J. (1967). Initial-Value Problem for the Motion in an Undulating Sea of a Body with Fixed Equilibrium Position. Journal of Engineering Mathematics, 1, 1-19.

Wehausen, J. & Laitone, E. (1960). Surface waves (9th ed.). Handbuch der Physik (ed. S. Flugge), Springer-Verlag.